Sortilin associates with Trk receptors to enhance anterograde transport and signaling by neurotrophins

Christian Bjerggaard Vaegter, Pernille Jansen, Anja Winther Fjorback, Simon Glerup, Sune Skeldal, Mads Kjolby, Mette Richner, Bettina Erdmann, Jens Randel Nyengaard, Lino Tessarollo, et al.

Sortilin associates with Trk receptors to enhance anterograde transport and neurotrophin signaling

by

Christian B. Vaegter[1], Pernille Jansen[1], Anja W. Fjorback[2], Simon Glerup[1], Sune Skeldal[1], Mads Kjolby[1], Mette Richner[1], Bettina Erdmann[3], Jens R. Nyengaard[2], Lino Tessarollo[4], Gary R. Lewin[3], Thomas E. Willnow[3], Moses V. Chao[5], and Anders Nykjaer[1,]

[1)] The Lundbeck Foundation Research Center MIND, Department of Medical Biochemistry, Ole Worms Allé 1170, Aarhus University, DK-8000 Aarhus C, Denmark, [2)] MIND Center, Stereology and Electron Microscopy Laboratory, Aarhus University, 8000 Aarhus C, Denmark, [3)] Max-Delbrück-Center for Molecular Medicine, 13125 Berlin, Germany, [4)] Center for Cancer Research, National Cancer Institute, Frederick, Maryland 21702, USA, [5)] Kimmel Center at Skirball Institute of Biomolecular Medicine, New York University School of Medicine, New York 10016, USA,

Correspondance: Anders Nykjaer, an@biokemi.au.dk
MIND Center, Department of Medical Biochemistry
Ole Worms Allé, Bldg. 1170
Aarhus University
DK-8000C Aarhus
Denmark
Fax: +45 8613 1160
Phone: +45 8942 2884

Christian B. Vaegter, cv@biokemi.au.dk
MIND Center, Department of Medical Biochemistry
Ole Worms Allé, Bldg. 1170
Aarhus University
DK-8000C Aarhus
Denmark

Binding of target-derived neurotrophins to Trk receptors at nerve terminals are required to stimulate neuronal survival, differentiation, innervation and synaptic plasticity. The distance between the soma and nerve terminal is tremendous, making efficient anterograde Trk transport critical for their synaptic translocation and signaling. The mechanism responsible for this trafficking remains poorly understood. Here we show that the sorting receptor sortilin interacts with TrkA, -B, and –C and enables their anterograde axonal transport, thereby enhancing neurotrophin signaling. Cultured DRG neurons lacking sortilin exhibit blunted MAPK signaling and reduced neurite outgrowth upon stimulation with NGF. Moreover, deficiency for sortilin considerably aggravates TrkA, -B- and –C phenotypes present in $p75^{NTR}$ knockouts, and results in increased embryonic lethality and sympathetic neuropathy in mice heterozygous for TrkA. Our findings demonstrate a novel and unexpected role for sortilin as an anterograde trafficking receptor for Trk and a positive modulator of neurotrophin-induced neuronal survival.

Neurotrophins are growth factors that are essential to regulate wiring of the nervous system during development, to ensure its maintenance in the adult organism, and to modulate synaptic transmission[1]. The growth factor family comprises nerve growth factor (NGF), brain-derived neurotrophic factor (BDNF), and neurotrophin-3 and -4, respectively, and they exert their trophic effects via binding to members of the tropomyosin-related kinase (Trk) receptors at the axon terminals of innervating neurons. NGF binds most specifically to TrkA, BDNF and neurotrophin-4 to TrkB, and neurotrophin-3 predominantly to TrkC but co-expression of the structurally unrelated $p75^{NTR}$ neurotrophin receptor refines the fidelity of the neurotrophins towards their cognate Trks, thereby augmenting trophic responses[1].

Trk receptors are produced at the cell body and rapidly propelled along the axonal shaft to the synapse by a process referred to as anterograde transport. Following neurotrophin-mediated activation, the receptors shuttle back from the axon terminals to the soma by retrograde transport in so-called signaling endosomes to regulate gene expression and exert their trophic responses[2]. While our understanding

of the retrograde trafficking process is becoming increasingly clear, the mechanisms underlieng anterograde Trk transport remain poorly understood. It is well established that axonal transport relies upon microtubule-based motor kinesin-proteins[3], an interaction that, at least for TrkB, can be mediated by an adaptor complex comprising Slp1/Rab27B and CRMP-2[4]. Yet, knockdown of any of these adaptors only reduces axonal targeting by 30-50% suggesting the existence of additional transport mechanisms.

Sortilin is one of five members of the Vps10p-domain family of sorting receptors[5]. It is abundantly expressed in neurons of the central and peripheral nervous systems. While only ~10% of sortilin is surface exposed, ~90% of the receptors are located in the TGN, endosomes, dendrites, axons, immature secretory granules, and synaptic vesicles[5-9]. Sortilin is capable of both rapid internalization, Golgi to endosome trafficking, retrograde transport to the TGN, and sorting into the pathway for regulated secretion; transport activities that are governed by binding of specific cytosolic adaptor proteins to the intracellular tail of the receptor[6, 7, 9]. The receptor is synthesized as an inactive precursor, pro-sortilin, that is incapable of ligand binding due to a propeptide that prevents ligands from entering the binding pocket[10]. In the trans-Golgi network (TGN) pro-convertase liberates this propeptide, rendering the receptor active[11].

We previously described that surface exposed sortilin can form a tripartite complex with $p75^{NTR}$ and secreted precursor forms of neurotrophins, denoted pro-neurotrophins (proNT), to induce cell death[12, 13]. However, prompted by the predominant intracellular localization of sortilin we speculated that the receptor might also engage in anterograde transport of Trks to the nerve endings. In accordance with this hypothesis we here report that sortilin surprisingly also facilitates trophic signaling by ensuring adequate Trk receptor expression at the synapse for mature neurotrophins to stimulate neuronal survival and differentiation.

Results

Sortilin physically interacts with Trk receptors

Immunofluorescence staining revealed that sortilin is frequently co-expressed with Trk and $p75^{NTR}$ in tissues, such as the adult dorsal root ganglia (DRG), which are not destined for apoptosis (**Fig. 1a**). This observation suggests additional functions for sortilin in neurotrophin action besides induction of apoptosis. Because sortilin is capable of intracellular sorting, we hypothesized that it might affect trafficking and the subcellular distribution of Trk receptors. To test this hypothesis, we subjected 293 human embryonic kidney (HEK) cells overexpressing sortilin and TrkA, –B and –C, respectively, to co-immunoprecipitation experiments using pan-anti-Trk or anti-sortilin antibodis. We found that sortilin can physically interact with all Trks (**Fig. 1b**, TrkB data in HEK cells not shown). Importantly, in addition to the mature 140 kDa TrkA receptor, also the immature and incompletely glycosylated 110 kDa precursor bound sortilin[14] (**Fig. 1b**).

A robust receptor-receptor interaction was substantiated by fluorescence resonance energy transfer (FRET) and fluorescence lifetime imaging microscopy (FLIM). We obtained a mean apparent pFRET efficiency Eapp of ≈8 % in cells expressing sortilin and TrkA (data not shown), while in FLIM imaging the average lifetime of the sortilin donor fluorophore decreased by ~100-300 ps when TrkA was present (**Fig. 1c**). The receptor interaction was furthermore demonstrated by surface plasmon resonance (SPR) analysis in which the extracellular domain of sortilin was immobilized on a sensorchip and soluble Trk ectodomains were present in the fluid phase. All Trks exhibited high affinity binding to sortilin with estimated Kd-values between 10 and 20 nM (**Fig. 1d**). Because ligand binding to sortilin is conditioned on the release of the receptor propeptide, we tested if Trk, as exemplified by TrkB, can bind to immobilized pro-sortilin (**Fig. 1d**). We found that pro-sortilin does not bind Trk, indicating that only the fully processed and mature receptor is capable of forming heterodimers with Trk. Moreover, binding of all Trk receptors to sortilin was prevented by co-incubation with the soluble sortilin propeptide (data not shown).

To ensure specificity of sortilin-Trk interaction, we tested if sortilin could bind an unrelated neurotrophin receptor, the glia-derived neurotrophic factor (GDNF) family ligand receptor Ret and one of its ligands neurturin[15]. We failed to detect any interaction of Ret and neurturin with sortilin, neither by co-immunoprecipitation (**Fig.**

1b) nor by SPR analysis (**Fig. 1d**), suggesting that the binding between sortilin and Trk receptors is specific.

In light of the above, we assessed if endogenous sortilin and Trk can interact in primary neurons. Because TrkB and sortilin are both expressed in hippocampal and cortical neurons, and these cells can be prepared in large quantities, we conducted co-immunoprecipitation experiments of lysates from such cultures. We found that TrkB robustly co-immunoprecipitated with sortilin from hippocampal (**Fig. 1e**) but also from cortical neurons (data not shown). Furthermore, immunofluorescence staining of non-transfected superior cervical ganglion (SCG) neurons revealed only occasional overlap in the expression pattern of sortilin and TrkA in the cell body (**Fig. 1f**). Yet, the receptors significantly co-localized in neurites, where they physically interacted as determined by a pFRET efficiency Eapp of 10-15%. We conclude that sortilin is capable of heterodimerization with Trk receptors in primary neurons of both the central and peripheral nervous system.

Sortilin facilitates anterograde Trk receptor transport

The heterodimerization of sortilin and Trk in neurites suggested that sortilin might affect transport properties of Trks in neuronal processes. To address this question cultured DRG neurons were transfected with EGFP-TrkA and the movement of vesicles expressing fluorescently labeled receptor was measured by time-lapse microscopy (**Figs. 2a** and **2b**, **Suppl. Movie 1** and **2**). Tracking of more than 350 vesicles from both wild-type and sortilin deficient (*Sort1*$^{-/-}$) neurons revealed that the ratio of measurable TrkA-positive vesicles moving anterograde was reduced by ~4 fold (from 21.9% to 4.9%) in knockout neurons (**Fig. 2c**). Contrary, fractions of vesicles moving retrograde or vesicles with no movement were identical in wild-type and knockout (KO) mice (**Fig. 2c**). The average vesicle speed in either direction was unaffected by sortilin expression, and amounted to approximately 0.6 μm/s for both genotypes (data not shown).

To examine if sortilin facilitates anterograde Trk transport in peripheral axons *in vivo* we performed sciatic nerve double ligations. Twenty four hours later, the nerves were removed and the proximal and distal regions probed for receptor expression. Sortilin strongly accumulated proximal (anterograde transport) as well distal (retrograde transport) to the ligature suggesting bi-directional axonal trafficking

(**Fig. 2d**). Next we extended these findings by comparing anterograde and retrograde transport of TrkA in the sciatic nerves of *Sort1*$^{+/+}$ (wild-type) and *Sort1*$^{-/-}$ mice (**Fig. 2e**). Remarkably, the mature 140 kDa form of TrkA was reduced by ~60% in the proximal region of the nerve in sortilin KO mice. Contrary, the immature and incompletely glycosylated 110 kDa variant of the protein was unaltered (**Figs. 2e** and **f**). Because p75^{NTR} trafficking was not affected in these experiments, as determined by comparable band intensities in wild-type and sortilin-deficient mice, we concluded that sortilin selectively assists in anterograde transport of mature TrkA. As a consequence of this trafficking deficit, *Sort1*$^{-/-}$ mice exhibited noticeable less TrkA in lysates of medial cerebral arteries, a target tissue for SCG neurons (**Fig. 2g**).

Prompted by the binding of sortilin and TrkB in cultured hippocampal neurons (**Fig. 1e**), we finally compared the subcellular distribution of TrkB in the hippocampus by performing membrane fractionation experiments (**Suppl. Fig. 1**). In the wild-type hippocampus, TrkB accumulated in synaptosomes and synaptic vesicles in accordance with previous findings[16]. However, in *Sort1*$^{-/-}$ mice the amount of TrkB was drastically reduced in these organelles, suggesting that efficient targeting of TrkB to the synapse requires sortilin (**Fig. 2h**).

Collectively, our data suggested that sortilin is capable of Trk binding in primary neurons and that this interaction is required for efficient anterograde transport and synaptic targeting of Trk receptors.

Impaired neurite outgrowth in cultured *Sort1*$^{-/-}$ neurons

Next we studied the impact of sortilin on TrkA function by investigating NGF signaling in cultured DRG neurons from wild-type and *Sort1*$^{-/-}$ mice. Immunoblotting confirmed that total TrkA levels in these cultures were unaffected by sortilin expression (**Suppl. Fig. 2**). Addition of 50 ng/ml NGF to wildtype neurons for 15 min induced activation of the MAP-kinases ERK1 and -2 (ERK1/2), a well-established downstream target of Trk activation (**Fig. 3a**)[17]. In contrast, phospho-ERK1/2 was attenuated by approximately 60% in *Sort1*$^{-/-}$ cultures despite identical levels of total ERK1/2, underscoring the importance of sortilin for efficient TrkA-mediated signaling (**Fig. 3a**–**b** and **Suppl. Fig. 2**). Since ERK1/2 phosphorylation is a key mediator of neurite outgrowth and differentiation of DRG neurons[17], we compared NGF-induced sprouting in primary DRG cultures from newborn mice. When cultured in the presence of low NGF

concentrations (25 ng/ml) for 12 hrs, knockout neurons exhibited a ~30% reduction in total neurite length, corroborating the critical role of sortilin for TrkA activity (**Fig. 3 c**–**d**). Importantly, 10-fold higher NGF concentrations (250 ng/ml) were able to overcome the impaired sprouting in the *Sort1*$^{-/-}$ neurons, suggesting that the number of surface exposed mature Trk receptors may be the primary cause of this defect (**Fig. 3d**).

We subsequently tested if impaired neurite outgrowth of *Sort1*$^{-/-}$ neurons was an intrinsic consequence of sortilin inactivation or whether it was specific for Trk-mediated stimulation. To this end, DRG cultures were stimulated with neurturin that signals through Ret[15]; a receptor that also undergoes anterograde transport[18]. As neither neurturin nor Ret physically interact with sortilin (**Figs. 1b** and **d**), one would predict the Ret/neurturin signaling pathway to be functionally unaffected by sortilin expression. Interestingly, we found no difference in sprouting between wild-type and *Sort1*$^{-/-}$ neurons at 100, 10 or even at 1 ng/ml neurturin (**Fig. 3e**), a concentration which is below the previously reported ED_{50} values of 2-10 ng/ml for sprouting and survival of primary neuronal cultures[19].

Taken together our data demonstrated that sortilin selectively impacts on Trk-dependent neuronal differentiation, suggesting that the heterodimerization between sortilin and Trk is biologically meaningful.

Sortilin supports neurotrophin activity *in vivo*

p75^{NTR} has a dual role in neurotrophin action as it induces apoptosis by proNTs in conjunction with sortilin[12] but also refines Trk affinity and specificity for their bona fide neurotrophins, thereby augmenting Trk signaling[1]. As a consequence, p75^{NTR} knockout mice - referred to as *Ngfr*$^{-/-}$ - exhibit phenotypes of reduced Trk signaling[20]. To distinguish between the effects of sortilin upon p75^{NTR} versus Trk receptors, we undertook an analysis of double knockout mice, reasoning that sortilin-dependent Trk signaling might be unmasked on the *Ngfr*$^{-/-}$ background.

In the first series of experiments, we intercrossed sortilin and p75^{NTR} double heterozygous mice to obtain mice deficient in both loci. Double knockout (DKO) mice were viable and born according to Mendelian ratio (**Suppl. Fig. 3**). Yet, starting about 4 weeks of age *Sort1*$^{-/-}$/*Ngfr*$^{-/-}$ mice showed a progressively abnormal waddling gait and an aberrant hind-limb posture (**Fig 4a**; **Suppl. movie 3**). Some

animals were also noticeable smaller than control littermates (**Suppl. Fig. 4**). The penetrance of this phenotype correlated with the number of knockout alleles, reaching 84% for the gait phenotype and 37% for the growth retardation in the DKO (**Table 1**). Because abnormal walking suggested a deficit in the peripheral nervous system, we quantified the number of myelinated fibers in the sciatic nerve as well as the neuronal profiles in the corresponding L4-L5 DRGs of animals 8 weeks of age (**Figs. 4b**–**c**). *Sort1*$^{-/-}$ mice did not show any decrease in the amount of myelinated fibers or DRG neurons despite a significant reduction in anterograde trafficking and functional activity (cf. **Figs. 2** and **3a**–**d**). The number of unmyelinated fibers was also similar and amounted to 2565+/–240 and 2712+/–481 for wild-type and sortilin-deficient animals, respectively. These observations are equivalent to Trk heterozygous mice that have 50% lower Trk levels, yet an unaltered number of DRG neurons[21-23].

In accordance with past findings[20, 24], we found that mice devoid in p75^{NTR} expression exhibited 35% fewer nerve fibers and a reduction in DRG neurons of ~50%. Interestingly, in the DKO both these values were further decreased by ~35% relative to *Ngfr*$^{-/-}$ mice (**Fig. 4b**–**c**), demonstrating that sortilin deficiency significantly impacts on neurotrophin signaling when p75^{NTR} is absent.

Loss of sortilin aggravates Trk phenotypes in *Ngfr*$^{-/-}$ mice

More than 70% of DRG neurons express sortilin and almost all p75^{NTR}- and Trk-positive neurons contain sortilin (**Fig 1a**). In agreement with literature, sortilin expression was not confined to a specific neuronal subpopulation within the DRG but present in all subtypes[25]. In detail, we found sortilin in nociceptive neurons including small unmyelinated (peripherin+) non-peptidergic (isolectin IB4+) and peptidergic (calcitonin gene-related peptide (CGRP)+, vanilloid receptor type-1 (TrpV1)+, TrkA+) neurons, and in medium-sized myelinated neurons that stain for neurofilament 200 (NF200) (data not shown). Larger diameter neurons that innervate cutaneous mechanoceptors and convey tactile sensation (TrkB+, NF200+) and large proprioceptive neurons that sense limb movement and position (TrkC+, NF200+) also possessed sortilin (data not shown). Thus, sortilin is expressed in neurons that subserve all perceptual somatic modalities.

Abnormal movement and posture has been described in mice lacking TrkC[26] or its ligand neurotrophin-3[27]. We therefore compared the number of

TrkC/NF200-expressing neurons in *Ngfr*$^{-/-}$ and *Sort1*$^{-/-}$/*Ngfr*$^{-/-}$ animals. We found that mice lacking p75^{NTR} exhibited a reduction in NF200- and TrkC-positive cells of approximately 36 and 42%, respectively. In the *Sort1*$^{-/-}$/*Ngfr*$^{-/-}$ these values were further reduced resulting in a total loss of ~60% of the TrkC-positive neurons (**Fig. 5a**). As a consequence of the attenuated proprioceptive innervation, muscle spindles were virtually absent in *Sort1*$^{-/-}$/*Ngfr*$^{-/-}$ mice (**Fig. 5b**). Collectively, our observations suggest that the profound reduction in TrkC-expressing sensory neurons in the *Sort1*$^{-/-}$/*Ngfr*$^{-/-}$ may account for the waddling gait and abnormal hind limb posture (cf. **Fig 4a**).

We next asked whether other neurotrophin phenotypes might also be affected in the sortilin/p75^{NTR} mutants. Mice heterozygous for BDNF show reduced mechanosensation and TrkB-deficiency is accompanied by loss of Merkel cells and Meissner's corpuscles[28, 28, 29, 29]. Hence, we subjected *Sort1*$^{-/-}$/*Ngfr*$^{-/-}$ mice to the Von Frey's test, a method used to assess mechanical nociception. Application of a force of 1.4 g induced 80-90% paw withdrawal response in wild-type and *Sort1*$^{-/-}$ animals but only a ~45% response in the p75^{NTR} knockouts. However, in *Sort1*$^{-/-}$/*Ngfr*$^{-/-}$ mice this value was reduced to less than 20% (**Fig. 5c**), suggesting an important modulatory role for sortilin in BDNF-dependent mechanosensation. In agreement with this notion, the number of TrkB-positive DRG neurons was decreased by ~20% in the DKO as compared to p75^{NTR}-null mice (**Fig. 5d**). This observation showed that even a modest reduction in TrkB-positive neurons dramatically affects the threshold of mechanical pain when the total decline in neurons exceeds ~50%.

TrkA-dependent unmyelinated afferents respond to heat-induced noxious stimuli[30]. To study if sortilin affects thermal algesia we subjected sortilin knockout mice to the Hargreaves test. Paw withdraw latencies were identical in wild-type and *Sort1*$^{-/-}$ animals but increased by 29% in p75^{NTR} knockouts in accordance with literature[20, 24] (**Fig. 6a**). However, an impact of sortilin on nociception was revealed on the *Ngfr*$^{-/-}$ background inasmuch as the latency was delayed by 72% in the DKO mice. In accordance with a TrkA phenotype[31], all subtypes of NGF-dependent nociceptors were significantly reduced in *Sort1*$^{-/-}$/*Ngfr*$^{-/-}$ when compared to *Ngfr*$^{-/-}$ littermates (**Fig. 6b**). Electron microscopy revealed that unmyelinated nociceptive axons, which are clustered in Remak bundles, had developed normally at postnatal day 15 (P15) (11.2+/−0.3 versus 10.1+/−0.5 neurons per bundle; data not shown) but later

underwent a dramatic degeneration (**Fig. 6c**). Out of 236 Remak bundles, 213 exhibited the abnormal morphology in the DKOs (n=5 mice). As a consequence of the degeneration and the impaired response to noxious stimuli, *Sort1*$^{-/-}$/*Ngfr*$^{-/-}$ mice displayed considerable mutilation or autotomy behavior that resulted in severe injury and deformity of their hindlimb paws after ~3 months of age[32] (**Fig. 6d**). In support of impaired TrkA-mediated signaling in double-deficient mice, we found that NGF-induced ERK1/2 phosphorylation was virtually abolished in DRG cultures from *Sort1*$^{-/-}$/*Ngfr*$^{-/-}$ mice (**Fig. 3a**–**b**).

TrkA heterozygosity is embryonic lethal in *Sort1*$^{-/-}$ mice

To investigate the specific genetic effects of sortilin upon Trk receptor function, we crossed the sortilin knockouts with mice heterozygous for a mutant TrkA allele (*Ntrk1*$^{+/-}$). Homozygous deficiency for TrkA is embryonic lethal[33] precluding the generation of DKO. Moreover, both genes are located on chromosome 3 approximately 20 cM apart, requiring allelic cross-over to produce offspring with three knockout alleles (**Fig. 7a**). Progeny from breeding pairs of *Sort1*$^{-/-}$/*Ntrk1*$^{+/+}$ and *Sort1*$^{+/-}$/*Ntrk1*$^{+/-}$ mice gave the expected equal frequency of double heterozygous (47%) and sortilin knockout offspring (40%), demonstrating that heterozygosity in the TrkA gene locus is not associated with reduced viability (**Fig.7b**). Contrary, on the *Sort1*$^{-/-}$ background, TrkA heterozygosity was accompanied by increased lethality. Thus, *Sort1*$^{-/-}$/*Ntrk1*$^{+/-}$ progeny, as a consequence of allelic cross-over, were born with a frequency of only 2.9% as compared to 8.6% for the equivalent *Sort1*$^{+/-}$/*Ntrk1*$^{+/+}$ genotype. This number corresponds to an embryonic excess lethality of ~65% for mice harboring three knockout alleles (**Fig.7b**). At day P27, this value had increased to 89% which show that *Sort1*$^{-/-}$/*Ntrk1*$^{+/-}$mice continue to die during the first weeks of life, mimicking the phenotype of the TrkA knockout mouse[33].

Because TrkA deficiency is also associated with a severe sympathetic neuropathy[33], we quantified the SCG volume in animals at P1. Previous studies in *Sort1*$^{-/-}$ did not reveal any obvious signs of impaired TrkA activity in SCG development[34]. However, in accordance with the lethal phenotype, *Sort1*$^{-/-}$/*Ntrk1*$^{+/-}$ mice had significantly smaller SCGs as compared to mice lacking only one functional TrkA allele (**Fig. 7c**).

Discussion

To assess the full biological functions of sortilin in neurotrophin signaling, we recently generated a sortilin-deficient mouse and confirmed that this receptor is indispensable for proNT-dependent death of neurons during certain stages of development, aging, and brain injury[34]. In this study, we used the same knockout mouse model to show that sortilin also facilitates neurotrophin signaling by escorting Trks along the axonal path to the synapse where receptor activation takes place.

In accordance with our previous findings, we did not observe any overt signs of reduced neurotrophin signaling in *Sort1*$^{-/-}$ animals[34]. Absence of trophic deficits *in vivo* is not surprising inasmuch as deficiency for sortilin reduces Trk anterograde transport and activity by approximately 40-50% (**Figs. 2** and **3a**–**d**), a value comparable to that present in TrkA, -B, and -C heterozygous mice that are also phenotypically normal[21-23]. In order to unmask a putative trophic function of sortilin, we therefore assessed the effects of sortilin on the *Ngfr*$^{-/-}$ background. We found that sortilin is required for full neurotrophin activity as receptor deficiency considerably aggravated the TrkA, -B, -C phenotypes present in *Ngfr*$^{-/-}$ mice.

During development Trk expression begins at day E13 in the DRG neurons and is readily apparent from E15[35]. Similarly, sortilin commences at embryonic day 14 and is maintained onward [36]. The simultaneous expression of the two receptors is compatible with a role for sortilin in Trk transport and signaling during development. However, several lines of evidence suggest that the DKO phenotype is due to neuronal degeneration rather than impaired development. Firstly, while motor skills of *Sort1*$^{-/-}$ /*Ngfr*$^{-/-}$ mice appeared normal at birth and during the first weeks of life, the waddling gait debuted at ~4 weeks of age when development of the peripheral nervous system has been completed. Secondly, at P15 the morphology of Remak bundles was normal in DKO mice and the number of non-myelinated neurons indistinguishable from those of *Ngfr*$^{-/-}$ animals. Yet, at ~8 weeks of age, Remak bundles in *Sort1*$^{-/-}$/*Ngfr*$^{-/-}$ animals had coalesced, whereas axons of the p75^{NTR} knockout mice remained unaffected (**Fig. 6c**). This degeneration was accompanied by reduced nociception which, in turn, lead to severe scaring and malformation of the paws (**Fig. 6d**). Collectively, these findings suggest that sortilin is particularly important for maintenance of the nervous system when the concentrations of neurotrophins become limited.

Co-immunoprecipitation demonstrated that both the immature and incompletely glycosylated 110 kDa TrkA and the mature 140 kDa form are capable of sortilin binding, suggesting that the binding interaction is independent of carbohydrate modifications (**Fig. 1b**). Yet, only the 140 kDa form was subject to sortilin-mediated transport in the sciatic nerve of *Sort1*$^{-/-}$mice (**Fig. 2e**–**f**). Interestingly, the inactive precursor of sortilin, pro-sortilin, was unable to bind Trk receptors. The presence of the propeptide prevents premature ligand binding to sortilin in the biosynthetic pathway but furin-mediated cleavage in the TGN conditions the receptor for full biological activity[11]. We therefore propose a model in which vesicles containing the incompletely glycosylated and high-mannose bearing 110 kDa Trk receptor segregates from the biosynthetic pathway in a compartment that precedes the late TGN where sortilin activation takes place (**Suppl. Fig. 5**). In accordance with such a model, Golgi outposts have been identified in distal dendrites, compatible with local glycosylation and maturation of the 110 kDa Trk receptor variants[37, 38]. The biological relevance of having two independent axonal targeting pathways for Trk receptors, of which one only is subject to sortilin-mediated transport remains to be elucidated.

Knockout of KLC-1, a subunit of the motor protein kinesin-1, is accompanied by reduced anterograde targeting of TrkA, suggesting an important role of this motor protein in Trk trafficking [39]. Indeed, a recent study demonstrated that an adaptor complex comprising Slp1/Rab27B/CRMP-2 directly links the cytoplasmic tail of Trk to kinesin-1[4]. Yet, knockdown of one or more of these adaptors reduced, but did not abrogate, anterograde Trk transport, membrane targeting and signaling. This suggests that alternative adaptor complexes, kinesin motors or sorting receptors may work in concert with kinesin-1 to escort Trk receptors to the synapse.

What could be the molecular mechanism by which sortilin facilitates Trk trafficking? Sortilin might act as a scaffold receptor that facilitates the formation of a higher order complex between Slp1/Rab27B/CRMP-2, kinesin-1, and Trk receptors. Alternatively, it could directly bridge Trk receptors with kinesin-1 or other microtubule motors. Interestingly, in a yeast-two-hybrid screening KIF1A, a subunit of kinesin-3 that transports synaptic vesicles, was identified as a sortilin interaction partner (personal communication: Dr. Peder Madsen, Aarhus University). Studies are in progress to evaluate the significance of this observation. Sortilin could also act upstream of the conventional anterograde transport machinery to ensure translocation

of Trks from the TGN into kinesin-dependent transport vesicles. Indeed, several observations support an important role of sortilin in regulating exit from the late Golgi compartments. For instance, sortilin has been shown to facilitate intracellular sorting of BDNF into the pathway for regulated secretion as well as to assist in assembly and export of very low density lipoprotein particles from the liver[9, 40].

Several cytoplasmic adaptor proteins for sortilin have been identified over the past and their functional roles characterized in terms of endocytosis and Golgi to endosome sorting [5]. Recently, one of these adaptors, phosphofurin acidic cluster-sorting protein 1 (PACS-1), which binds to an acidic cluster in the cytosolic domain of sortilin, was shown also to mediate anterograde transport in polarized cells[5, 41]. Thus, overexpression of a dominant-negative PACS-1 variant revealed that this adaptor is required for trafficking of the olfactory cyclic-nucleotide-gated channel from the cell body to the microtubule based cilia of the apical dendrite in olfactory sensory neurons[41]. Whether PACS-1 is also required for anterograde transport of sortilin is currently under investigation.

Finally, axonal Trk targeting has been suggested to be accomplished by a more circuitous trafficking pathway than classically appreciated[42]. According to this transcytosis model, Trk receptors are initially embedded into the plasma membrane of the neuronal soma from where they are constitutively endocytosed and axonally propelled via recycling endosomes. Because sortilin is being avidly internalized, a role for this receptor in Trk transcytosis could be envisioned. However, with the reservation of having used non-polarized cells, we did not observe any reduction in Trk surface expression in 293HEK cells stably transfected with sortilin (data not shown). Since constitutive internalization is considered independent on cell polarity, we find it unlikely that sortilin is accountable for the Trk transcytosis.

In conclusion, our data have unraveled sortilin as an important anterograde trafficking receptor for the Trks. We propose a new tripartite model for neurotrophin signaling which we have named the 'neurotrophin triangle' (**Suppl. Fig. 6**): Sortilin is essential for proneurotrophins to form a death signaling complex with $p75^{NTR}$ [12, 34]. Signaling by Trks, on the other hand, requires $p75^{NTR}$ expression at the plasma membrane to facilitate binding of mature neurotrophins and to strengthen the trophic signals[1]. To complete this triangular interaction cascade, we have here shown

that sortilin supports and fine-tunes neuronal survival by facilitating the anterograde transport of Trk receptors and securing their proper exposure in the synapse.

Acknowledgements

This work was supported by the Lundbeck Foundation, The Danish Medical Research Council, Elvira and Rasmus Rissforts Foundation, MEMORIES (EU, Framework Programme 6), NIH (NS21072 and AG025970), the DFG, Danish Council for Strategic Research, Center for Stochastic Geometry and advanced Bioimaging (Villum Foundation), and by grants from the NIH (NS21072 and HD23315).

Author contributions

C.B.V., P.J., A.W.F., S.G., S.S., M.R., M.K. and B.E. conducted the experiments. J.R.N, L.T., G.R.L., T.E.W. and M.V.C. provided reagents and scientific input. C.B.V. and A.N. designed the experiments and evaluated the data, and C.B.V. and A.N. wrote the manuscript.

Figure Legends

Figure 1 Sortilin interacts with Trk receptors. **a**, Co-localization of sortilin with $p75^{NTR}$ and Trk receptors in DRG neurons. **b**, *Left:* co-immunoprecipitation of sortilin and TrkA in HEK293 using pan-anti-Trk or anti-sortilin antibody, respectively (IP), *Middle:* co-immunoprecipitation of sortilin with TrkC in HEK293 using pan-anti-Trk (IP), *Right:* No co-immunoprecipitation of sortilin with Ret. Proteins are visualized by western blotting. **c**, Interaction between sortilin and TrkA in HEK293 cells as measured by reduction in donor fluorophore Alexa488 (sortilin) lifetime (FLIM) in the presence of the acceptor fluorophore Alexa568 (TrkA). **d**, Surface plasmon resonance analysis of receptor interactions. *Upper panel:* Binding of extracellular domains of TrkA and –C, but not of Ret and neurturin (NRTN), to immobilized sortilin ectodomain. *Lower panel:* Binding of TrkB to sortilin but not to pro-sortilin (*red curve*). **e**, co-immunoprecipitation of TrkB from hippocampal neurons by anti-sortilin antibody but not by pre-immune IgG. **f**, Immunofluorescence staining of endogenous sortilin and TrkA in cultured SCG neurons. pFRET signal of co-localized receptors was obtained in neurites *(bottom right)*. Panels b and e contain cropped blots; full-length blots are presented in Supplementary Figure 7.

Figure 2 Endogenous sortilin facilitates neuronal Trk trafficking. **a**, Movement of EGFP-TrkA in neurites of cultured DRG neurons. Arrows indicate anterograde *(red)* and retrograde *(yellow)* movement of vesicles. **b**, Kymograph of a neurite as shown in panel a. Images were captured every 2 s for 300 s per neurite and kinetic parameters for each vesicle trace obtained by ImageJ KymoToolBox analysis. **c**, Relative frequencies of anterograde, retrograde or no movement of approximately 350 TrkA-positive vesicles of each genotype as described in b (mean +/– s.e.m.) **d**, Immunofluorescence of sortilin *(red)* and DAPI staining *(blue)* of a double ligated rat sciatic nerve. Accumulation of sortilin proximal and distal to the ligation illustrating anterograde and retrograde sortilin transport, respectively. **e**, western blot of double ligated sciatic nerves in wild-type and sortilin-deficient mice; anterograde TrkA transport *(top)*, bidirectional transport of $p75^{NTR}$ *(middle)* and actin loading control *(bottom)* based on intensity of immunoreactive protein bands proximal (P) and/or

distal (D) to the ligature. **f**, Quantification of anterogradely transported mature and immature TrkA in sortilin KOs relative to wild-type mice determined by densitometric scanning, cf. panel e (n=3; mean +/− s.e.m.). **g**, Western blot of middle cerebral arteries from two representative experiments (#1 and #2) illustrating reduced peripheral TrkA targeting in *Sort1*$^{-/-}$ mice. **h**, Western blot analysis of TrkB in hippocampal subcellular fractions from two representative experiments (#1 and #2) showing reduced TrkB in synaptic fractions (boxed in red) from *Sort1*$^{-/-}$ mice (n=4). P1: initial precipitation, S1: Initial supernatant, P2: Crude synaptosomes, S2: Light membrane; cf. Suppl. Fig. 1. Panels e, g and h contain cropped blots; full-length blots are presented in Supplementary Figure 7.

Figure 3 Sortilin facilitates Trk signaling in neurons. **a**, Western blot of phospho-ERK1/2 (MAPK) in primary DRG neuron cultures after stimulation with NGF for 10 min. **b**, Quantification of ERK1/2 activation from 5 experiments as depicted in panel a (mean +/− s.e.m.). **c**, TUJ-1 staining of DRG neurons 12h after plating. **d, e**, Quantification of neurite length (n=4) after stimulation with NGF *(panel d)* or the Ret ligand neurturin *(panel e)* (mean +/− s.e.m.). Panel a contains a cropped blot; the full-length blot is presented in Supplementary Figure 7.

Figure 4 Aberrant gait and peripheral neuropathy in sortilin and p75^{NTR} double knockout mice **a**, Abnormal hind-limb posture in *Sort*$^{-/-}$/*Ngfr*$^{-/-}$ mice. **b**, Quantification of myelinated axons in the sciatic nerve (*left,* mean +/− s.e.m.) and nerve morphology (*right*). **c**, Number of neurons in adult L4 and L5 DRGs (n=4) (mean +/− s.e.m.).

Figure 5 Loss of sortilin aggravates TrkC and TrkB phenotypes in p75^{NTR} knockout mice. **a**, Quantification of proprioceptive neurons in L4/L5 DRGs using markers for NF200 and TrkC (n=8) (mean +/− s.e.m.). **b**, Reduced number of muscle spindles in hind-limbs from P1 *Sort1*$^{-/-}$/*Ngfr*$^{-/-}$ mice. **c**, von Frey stimulus-response curves from 10 wild-type, 8 *Sort1−/−*, 7 *Ngfr−/−* and 6 DKO mice. p-values for *Sort1*$^{-/-}$ and *Ngfr*$^{-/-}$ are relative to wild-type, and *Sort*$^{-/-}$/*Ngfr*$^{-/-}$ are relative to *Ngfr*$^{-/-}$ (curve) (mean +/− s.e.m.). **d**, Numbers of TrkB positive DRG neurons in adult mice (n=8) (mean +/− s.e.m.).

Figure 6 Sortilin deficiency aggravates TrkA phenotypes in $p75^{NTR}$ knockout mice. **a**, Thermal response as measured by Hargreaves test (n=10) (mean +/– s.e.m.). **b**, Quantification of nociceptive neuron subtypes in L4-L5 DRG (n=8) (mean +/– s.e.m.). **c**, Electron micrographs showing the morphology of Remak bundle fibers in adult and P15 mice. **d**, Hind limb degeneration in DKO at 3-4 month of age.

Figure 7 Absent sortilin expression induces TrkA phenotypes in *Ntrk1*$^{+/-}$ mice. **a**, Schematic representation of possible genotypes of offspring from *Sort1*$^{+/-}$/*Ntrk1*$^{+/-}$ and *Sort1*$^{-/-}$/*Ntrk1*$^{+/+}$ breeding pairs. **b**, Genotype frequency of offspring at P1 *(left side of dashed line)* and excess lethality of *Sort1*$^{-/-}$/*Ntrk1*$^{+/-}$ over *Sort1*$^{+/-}$/*Ntrk1*$^{+/+}$ offspring at P1 and P28 *(right side of dashed line)*, cf. panel a. **c**, SCG volume in newborns of the indicated genotypes (mean +/– s.e.m.).

Table 1

Genotype		Phenotypes			
Sortilin	$p75^{NTR}$	Waddling gait			Growth retardation
		Present	Moderate	Severe	
(+/+)	(+/+)	0% (0/8)			
(+/–)	(+/+)	0% (0/5)			
(–/–)	(+/+)	0% (0/7)			
(+/+)	(+/–)	0% (0/20)			
(+/–)	(+/–)	0% (0/10)			
(–/–)	(+/–)	12% (6/52)	12% (6/52)		
(+/+)	(–/–)	9% (1/11)	9% (1/11)		
(+/–)	(–/–)	29% (4/14)	7% (1/14)	21% (3/14)	7% (1/14)
(–/–)	(–/–)	84% (32/38)	34% (13/38)	50% (19/38)	37% (14/38)

Table 1 Correlation between genotype and penetrance of the various phenotypes. Parenthesis indicates affected animals out of the total number of mice in each group.

Methods

Animals. *Sort1*$^{-/-}$, *Ngfr*$^{-/-}$, and *Ntrk1*$^{-/-}$ mice have been described previously[20, 33, 34]. DKO were generated by breeding of double heterozygous animals and littermates served as controls. Results obtained on a pure C57BL/6J genetic background and on hybrid 129SvEmcTer X C57BL/6J and 129SvEmcTer X BALB/cJ lines were similar. Animal experimentation was performed according to good laboratory practice in full compliance with Danish and European regulations. All experiments were approved by the Danish Animal Experiments Inspectorate under the Ministry of Justice (permission number: 2006/561-1206).

Middle Cerebral Artery (MCA). MCAs were dissected from 10-13 animals of each genotype. The tissue was homogenized and lysed and separated by SDS-PAGE, followed by western blotting and incubation with anti-TrkA (Reichardt anti-TrkA, described below). Bands were visualized by ECL femto reagents (Pierce). Actin was used to control equal amounts of loaded protein between genotypes.

Neuron cultures: DRG and SCG cultures were prepared from P0-P3 mice by digesting the isolated ganglia in trypsin (0.125%) and collagenase (1 mg/ml), followed by seeding on PLL/laminin in DMEM supplemented with 10% FCS, 1mM glutamine, Primocin (Amaxa), 20 µM 5-Fluoro-2′-deoxyuridine, 20 µM Uridine and 2 nM NGF. Hippocampus neurons were prepared from P0 mice by digestion with papain (20 units/ml) for 30min, followed by seeding on PLL/laminin in neurobasal supplemented with B27, glutamax and primocin.

FRET/FLIM: Dissociated SCG neurons as well as HEK293 cells stably expressing sortilin or sortilin+TrkA[12] were incubated with goat anti-sortilin (R&D) and rabbit anti-Trk (RTA, L. Reichardt, UCSF) followed by Alexa-conjugated donkey secondary antibodies (anti-goat Alexa488 and anti-rabbit Alexa 568). Samples were analyzed on a Zeiss confocal LSM 510 META microscope using a 40x NA 1.2 C-Apochromat (HEK293) or 63x NA 1.4 Plan-Apochromat objective (SCG). FRET: Sensitized acceptor emission FRET were performed as described[43]. Briefly, Donor and acceptor signals were detected through 500-530 nm and 565-615 nm emission filters following 488 nm (donor) or 543nm (acceptor) excitation, respectively. The collected FRET images were analyzed by ImageJ-based PFRET software, enabling us to correct for donor- and acceptor spectral bleedthroughs (DSBT and ASBT) on donor- and acceptor signal levels. All calculations/corrections were performed on background-subtracted images.

Lower bounds for signal levels used in ASBT and DSBT correction calculations were set to 25. ROI's were chosen to be 5X5 and only ROI signal levels ≥20 for all pixels in the ROI's were included for analysis. Measurements were performed on 30 HEK293 cells and 10 SCG neurons. FLIM: The microscope was equipped with a mode-locked Ti-sapphire laser (Mai-Tai Broadband, Spectra Physics), photon counting card (SPC830), detector and software from Becker and Hickl (SPCM v. 2.9.4.1993). Alexa488 was two-photon excited with 20mW at 760 nm and the fluorescence detected after reflection off a 535DCXR dichroic (Chroma) and transmission through ET505/40m-2p and E700SP-2p filters (Chroma). Fluorescence decay curves measured for Alexa488 (Sortilin) in the presence and absence of Alexa568 (TrkA) were fitted to mono-exponential decay functions in SPCImage, using bin 1, amplitude threshold 50, scatter parameter fixed to 0, leaving all other parameters free. The instrument response function was calculated automatically by SPCImage. Histograms with lifetime as well as Chi-square value distributions obtained from the fitted pixels were generated by the software, depicted as pixel intensity weighted, and the mean lifetime and mean Chi-square value of each distribution was evaluated for each data file. Measurements were performed on 16 HEK293 cells.

MAPK activation assay. 10-12 DIV DRG cultures were washed 4x 1h in 37°C DMEM followed by incubation for 15 min at 37°C with DMEM + 2 nM NGF. The cells lysate (lysis buffer: 20 mM Tris pH 8, 1% NP40, 10mM EDTA, complete protease inhibitor cocktail (Roche), 2mM sodium orthovanadate and phosphatase inhibitor cocktail 1 (Sigma)) was subjected to SDS-PAGE (equal amounts of protein loaded), blotted, probed with anti-phospho-p42/44 MAP kinase (P-MAPK) antibody (Cell Signaling) and HRP-conjugated secondary antibody (Dako) and visualized with ECL substrate (Pierce). Equal loading was verified by blotting against beta-actin. Densitometry analysis of bands was performed using Multi Gauge 3.0 software (FujiFilm Life Science). NGF stimulated increase in P-MAPK was normalized to control within each experiment (n=3).

Neurite outgrowth

DRG neurons from P0-P1 mice were incubated with NGF (1 or 10 nM) or Neuturin (1, 10 or 100 ng/ml) for 12h, fixed and incubated with TUJ-1 primary antibody (Chemicon) followed by Alexa488-conjugated secondary antibody (Molecular probes). Images of complete branches were quantified by NeuriteTracer plugin for ImageJ

software (>20 neurons per experiment for each genotype). Average total length per neuron was calculated and the mean value for each experiment normalized to wild-type (n=4 to 6)

Live cell imaging. P0 DRG neurons were transfected (Amaxa) with EGFP-TrkA and seeded in MatTek glass-bottom chamber. The following day the cells were depleted of NGF for 6h and placed in a CO_2/temperature incubator attached to the microscope. Movies were recorded on a Zeiss LSM510 63x/1.4 oil objective and 30 frames per minute setting. A total of 350 vesicles were analyzed for each genotype in 8-10 neurons prepared in 3 independent experiments. Vesicle movement were analyzed with ImageJ using the KymoToolBox plugin (kindly provided by Fabrice Cordelières, Université Paris-Sud Orsay - France).

Surface Plasmon Resonance. SPR analysis were performed on a Biacore®3000 as previously described[12]. Briefly, soluble sortilin was immobilized (at 10–15 µg/ml) on a CM5 chip and remaining coupling sites were blocked with 1 M ethanolamine. Sample and running buffer was 10 mM HEPES, 150 mM $(NH_4)_2SO_4$, 1.5 mM $CaCl_2$, 1 mM EGTA, 0.005% Tween-20 pH 7.4. Fc-fusions proteins of $p75^{NTR}$, RET, TrkA, -B and -C (R&D Biotechnology) were applied at 20, 100 and 500 nM in increasing concentration, and the sensor chip regenerated in a 10 mM glycine-HCl buffer after each analytic cycle. The SPR signal was expressed in relative response units (RU) as the response obtained in a control flow channel was subtracted.

Immunoprecipitation. HEK293 cell lines stably expressing combinations of sortilin and TrkA or C or RET as well as dissociated hippocampus and cortical cultures were treated with DSP crosslinker (Pierce Biotechnology), lysed in TNE lysis buffer (20 mM Tris pH 8, 1% NP40, 10mM EDTA, complete protease inhibitor cocktail) and the cell lysate immunopreciptated with anti-Trk antibody (C14, Santa Cruz Biotechnology) or polyclonal anti-sortilin antibody linked to sepharose G beads (Amersham Biosciences). For neuronal cultures, control IP was performed with rabbit pre-immune serum. Following elution, SDS-PAGE and blotting, the proteins were probed with anti-sortilin (BD Transduction Labs), anti-Trk (C14, Santa Cruz Biotechnology), anti-TrkB or anti-Ret (R&D Systems) and visualized with HRP-conjugated secondary antibody (Dako) and ECL substrate (Pierce).

Hippocampus subcellular fractionation. The procedure for preparation of hippocampal synaptosomes was performed essentially as described by Blackstone et

al[44]. In brief, hippocampus was isolated from 12 wild-type or *Sort1*$^{-/-}$ mice (12-16 weeks old) and homogenized in 0.32 sucrose, 4 mM Hepes, pH 7.4 containing proteinase inhibitors. For each experiment, wild-type and *Sort1*$^{-/-}$ samples were processed in parallel in order to directly compare fractions (n=4). P1 and S1 are the pellet and supernatant, respectively, after centrifugation for 10 min at 1,000 × g. S1 was further centrifuged for 15 min at 10,000 × g to obtain supernatant S2 (light membranes) and the pellet P2, a crude synaptosomal preparation. Solubilized P2 was centrifuged for 15 min at 10,000 × g and the resulting pellet was solubilized in ice cold H_2O using a glass-teflon homogenizer and centrifuged again at 25,000 × g for 20 min generating the synaptosomal membrane fraction P3 and a supernatant S3 enriched in presynaptic vesicles. All centrifugation steps were performed at 4°C. Total protein concentration in fractions was determined using the Bicinchoninic Acid kit from Sigma and equal amounts of proteins of each fraction was separated by reducing SDS-PAGE and analyzed by western blotting for the presence of TrkB and synaptophysin.

Immunohistochemistry: L4/L5 DRG was fixed in 4% PFA, cryoprotected in 25% sucrose, embedded in TissueTek® and cut (14µm) on a cryostat, thaw-mounted on Superfrost Plus slides and kept at -80°C until use. After antigen retrieval (0.05% tween20 in 10 mM citrate buffer, pH 6.0 at 95°C for 20 min) and blocking (5% goat serum + 0.3% TritonX100) the tissue was incubated with antibodies against peripherin (Abcam), heavy neurofilament 200 (Abcam), TrpV1 (Neuromics), TrkA (L. Reichardt, UCSF), TrkB (Santa Cruz), TrkC (R&D), CGRP (Biomol), p75^{NTR} (9651)[45] or sortilin (Alomone labs). Alexa-conjugated secondary antibodies were obtained from Molecular Probes Inc. IB4-reactive neurons were visualized by IB4-FITC (Sigma-Aldrich L2895, 10 µg/ml). Images were recorded on a Zeiss LSM510 confocal microscope. For neuron profile estimation, every 3rd section was stained with cresyl violet and the total number of neuronal profiles with nucleoli counted in L4 and L5 DRG. Method validity was verified by several control experiments, e.g. comparing p75$^{NTR-/-}$ counts from adult mice with published data obtained by the design-based optical fractionator principle, yielding identical results (47.2 +/- 3.0% versus 47.9 +/- 7.7% of wild-type, respectively). Quantification of neurons positive for molecular markers was achieved by counting positive and total neuron profiles on at least 20

independent (non-adjacent) sections (more than 10 DRGs per genotype evaluated in total). Marker distributions for the wild-type were performed as described[24, 46-48].

Histology of sciatic nerve: N. Ischiadicus was dissected from adult mice, fixed in 4% PFA, incubated in 1% osmiumtetroxide in cacodylate buffer, dehydrated in increasing ethanol gradient (30%-99%), incubated in Technovit 7100 + Hardener I and finally embedded in Technovit 7100 + Hardener II (Kulzer, Germany). Tissue blocks were sectioned (3 µm), stained with Toluidin Blue (TB) and number of myelinated axons counted.

Electron microscopy: The sciatic nerve was dissected and processed as described previously[49]. Briefly, tissue from transcardially perfusion fixed mice (4% PFA) was postfixed in 4% PFA+ 2.5% glutaraldehyde. Following treatment with 1% osmium tetroxide they were dehydrated in a graded ethanol series and propylene oxide and embedded in Poly/BedR 812 (Polysciences, Inc., Eppelheim, Germany). Semithin sections were stained with toluidine blue. Ultrathin sections (70 nm) were contrasted with uranyl acetate and lead citrate and examined with a Zeiss 910 electron microscope. Digital images were taken with a high-speed slow scan CCD camera (Proscan) at an original magnification of 1250x and 5000x.

Sciatic nerve ligation. Adult mice were anaesthetized with ketamine/xylazine and the right sciatic nerve was double ligated at mid-high level. After 24h the animals were sacrificed and 3-4mm sciatic nerve proximal and distal to the ligation (or approximately at the same location for control side) was isolated. Nerve segments from 8-10 animals of each genotype were pooled for each experiment (3 independent experiments) and homogenized/lysed in lysis buffer (as for MAPK activation assay). 100µg protein per lane was separated by SDS-PAGE and western blotting, followed by incubation with anti-TrkA, anti-$p75^{NTR}$ or anti-sortilin (antibodies as described above) followed by HRP-conjugated secondary antibody. Densitometry analysis was performed using Multi Gauge 3.0 software and band intensity normalized to wild-type for each western blot.

Behavioral tests. Animals were kept under a 12h/12h day/might cycle and had unrestricted access to water and food. On the day of the experiment unrestrained animals were allowed to habituate for 1 hour before start of the experiments.

Hargreaves test: The radiant heat source (37380, Ugo Basile) was calibrated using a Heat Flow I.R, Radiometer (37300, Ugo Basile) and kept at 50% (190 mW/cm^2) in all

tests. The hind paws were tested alternately with >5 minutes between consecutive tests, and 3-5 measurements were obtained for each side. 10-14 animals were tested.
Von Frey test: Von Frey hairs of increasing bending force (calibrated 0.008g – 1.4g from Touch-Test® Sensory Evaluators, North Coast Medical, CA) were each applied 5 times to both sides of the plantar hind limb area from below through the mesh floor, and the number of withdrawals counted.

SCG volume. SCG ganglia from P28 mice fixed in 4% PFA and cryo-sectioned (20 µm) were incubated with anti-tyrosine hydroxylase antibody (Pel Freeze), followed by biotinylated anti-rabbit-IgG (Amersham) and Streptavidin-HRP-conjugated (DakoCytomation), visualized by DAB and the samples dehydrated and mounted in Eukitt. SCG neurons were photographed (Leica LM50) and the individual volume estimated by the principle of Cavalieri as described previously[34].

Muscle spindle. The lower hind legs of neonatal mice were snap frozen in isopentane and cryosectioned transversely at 10-12 µm. Every 6th section were incubated with antibody S46 (DSHB) as a marker for slow tonic myosin heavy chain (MHCst) intrafusal fibers located in muscle spindles[50]. The tissue were preincubated with goat anti-mouse Fab fragments (Jackson labs) to reduce unspecific binding of the secondary antibody, followed by HRP-conjugated rabbit anti-mouse (Dako) and visualized with DAP. Qualitative estimation of spindle numbers and size were obtained upon examination using an x4 objective (Leica microscope).

Statistical analysis. Statistical significance was determined by 2-tailed student's t-test or ANOVA after testing for normal distribution when appropriate. One-sample tests were applied to quantification from DRG neurite outgrowth, MAPK phosphorylation assay as well as sciatic TrkA transport. Breeding outcome was evaluated by Chi-square test.

Methods Reference list:

12. Nykjaer,A. *et al.* Sortilin is essential for proNGF-induced neuronal cell death. *Nature* **427**, 843-848 (2004).

20. Lee,K.F. *et al.* Targeted mutation of the gene encoding the low affinity NGF receptor p75 leads to deficits in the peripheral sensory nervous system. *Cell* **69**, 737-749 (1992).

24. Bergmann,I. *et al.* Analysis of cutaneous sensory neurons in transgenic mice lacking the low affinity neurotrophin receptor p75. *Eur. J. Neurosci.* **9**, 18-28 (1997).

33. Smeyne,R.J. *et al.* Severe sensory and sympathetic neuropathies in mice carrying a disrupted Trk/NGF receptor gene. *Nature* **368**, 246-249 (1994).

34. Jansen,P. *et al.* Roles for the pro-neurotrophin receptor sortilin in neuronal development, aging and brain injury. *Nat. Neurosci.* **10**, 1449-1457 (2007).

43. Wallrabe,H., Elangovan,M., Burchard,A., Periasamy,A., & Barroso,M. Confocal FRET microscopy to measure clustering of ligand-receptor complexes in endocytic membranes. *Biophys. J.* **85**, 559-571 (2003).

44. Blackstone,C.D. *et al.* Biochemical characterization and localization of a non-N-methyl-D-aspartate glutamate receptor in rat brain. *J. Neurochem.* **58**, 1118-1126 (1992).

45. Huber,L.J. & Chao,M.V. Mesenchymal and neuronal cell expression of the p75 neurotrophin receptor gene occur by different mechanisms. *Dev. Biol.* **167**, 227-238 (1995).

46. Chen,C.L. *et al.* Runx1 determines nociceptive sensory neuron phenotype and is required for thermal and neuropathic pain. *Neuron* **49**, 365-377 (2006).

47. Holmes,F.E. *et al.* Targeted disruption of the galanin gene reduces the number of sensory neurons and their regenerative capacity. *Proc. Natl. Acad. Sci. U. S. A* **97**, 11563-11568 (2000).

48. Zwick,M. *et al.* Glial cell line-derived neurotrophic factor is a survival factor for isolectin B4-positive, but not vanilloid receptor 1-positive, neurons in the mouse. *J. Neurosci.* **22**, 4057-4065 (2002).

49. Wetzel,C. *et al.* A stomatin-domain protein essential for touch sensation in the mouse. *Nature* **445**, 206-209 (2007).

50. Sokoloff,A.J., Li,H., & Burkholder,T.J. Limited expression of slow tonic myosin heavy chain in human cranial muscles. *Muscle Nerve* **36**, 183-189 (2007).

Supplementary Information Titles

Please list each supplementary item and its title or caption, in the order shown below. Please include this form at the end of the Word document of your manuscript or submit it as a separate file.

Note that we do NOT copy edit or otherwise change supplementary information, and minor (nonfactual) errors in these documents cannot be corrected after publication. Please submit document(s) exactly as you want them to appear, with all text, images, legends and references in the desired order, and check carefully for errors.

Journal: Nature Neuroscience

Article Title:	Sortilin associates with Trk receptors to enhance anterograde transport and neurotrophin Signaling
Corresponding Author:	Christian B. Vaegter and Anders Nykjaer

Supplementary Item & Number **(add rows as necessary)**	Title or Caption
Supplementary Figure 1	Hippocampal membrane fractionation. Schematic overview of sample preparation.
Supplementary Figure 2	Lysates of cultured DRG neuron immunoblotted for TrkA, Erk1/2, and actin as a loading control
Supplementary Figure 3	Genetic variation of offspring from intercrossing of mice double heterozygous for sortilin and $p75^{NTR}$ ($Sort^{+/-}/Ngf^{+/-}$)
Supplementary Figure 4	Growth retardation in 6 weeks old $Sort^{-/-}/Ngf^{-/-}$ mice.
Supplementary Figure 5	Schematic model describing sortilin in Trk trafficking
Supplementary Figure 6	Schematic model of the 'Neurotrophin triangle' concept
Supplementary Figure 7	Full-length gels of main article figures
Supplementary Video 1	Live cell imaging of a wt DRG neuron transfected with EGFP-TrkA
Supplementary Video 2	Live cell imaging of a $Sort1^{-/-}$ DRG neuron transfected with EGFP-TrkA
Supplementary Video 3	Characteristic waddling gate in sortilin and $p75^{NTR}$ double knockout mouse.

Reference List

1. Chao,M.V. Neurotrophins and their receptors: a convergence point for many signalling pathways. *Nat. Rev. Neurosci.* **4**, 299-309 (2003).

2. Hirokawa,N., Noda,Y., Tanaka,Y., & Niwa,S. Kinesin superfamily motor proteins and intracellular transport. *Nat. Rev. Mol. Cell Biol.* **10**, 682-696 (2009).

3. Hirokawa,N. & Takemura,R. Molecular motors and mechanisms of directional transport in neurons. *Nat. Rev. Neurosci.* **6**, 201-214 (2005).

4. Arimura,N. *et al.* Anterograde transport of TrkB in axons is mediated by direct interaction with Slp1 and Rab27. *Dev. Cell* **16**, 675-686 (2009).

5. Willnow,T.E., Petersen,C.M., & Nykjaer,A. VPS10P-domain receptors - regulators of neuronal viability and function. *Nat. Rev. Neurosci.* **9**, 899-909 (2008).

6. Nielsen,M.S. *et al.* The sortilin cytoplasmic tail conveys Golgi-endosome transport and binds the VHS domain of the GGA2 sorting protein. *EMBO J.* **20**, 2180-2190 (2001).

7. Petersen,C.M. *et al.* Molecular identification of a novel candidate sorting receptor purified from human brain by receptor-associated protein affinity chromatography. *J. Biol. Chem.* **272**, 3599-3605 (1997).

8. Sarret,P. *et al.* Distribution of NTS3 receptor/sortilin mRNA and protein in the rat central nervous system. *J. Comp Neurol.* **461**, 483-505 (2003).

9. Chen,Z.Y. *et al.* Sortilin controls intracellular sorting of brain-derived neurotrophic factor to the regulated secretory pathway. *J. Neurosci.* **25**, 6156-6166 (2005).

10. Quistgaard,E.M. *et al.* Ligands bind to Sortilin in the tunnel of a ten-bladed beta-propeller domain. *Nat. Struct. Mol. Biol.* **16**, 96-98 (2009).

11. Munck,P.C. *et al.* Propeptide cleavage conditions sortilin/neurotensin receptor-3 for ligand binding. *EMBO J.* **18**, 595-604 (1999).

12. Nykjaer,A. *et al.* Sortilin is essential for proNGF-induced neuronal cell death. *Nature* **427**, 843-848 (2004).

13. Teng,H.K. *et al.* ProBDNF induces neuronal apoptosis via activation of a receptor complex of p75NTR and sortilin. *J. Neurosci.* **25**, 5455-5463 (2005).

14. Martin-Zanca,D., Oskam,R., Mitra,G., Copeland,T., & Barbacid,M. Molecular and biochemical characterization of the human trk proto-oncogene. *Mol. Cell Biol.* **9**, 24-33 (1989).

15. Runeberg-Roos,P. & Saarma,M. Neurotrophic factor receptor RET: structure, cell biology, and inherited diseases. *Ann. Med.* **39**, 572-580 (2007).

16. Gomes,R.A., Hampton,C., El-Sabeawy,F., Sabo,S.L., & McAllister,A.K. The dynamic distribution of TrkB receptors before, during, and after synapse formation between cortical neurons. *J. Neurosci.* **26**, 11487-11500 (2006).

17. Reichardt,L.F. Neurotrophin-regulated signalling pathways. *Philos. Trans. R. Soc. Lond B Biol. Sci.* **361**, 1545-1564 (2006).

18. Russell,F.D., Koishi,K., Jiang,Y., & McLennan,I.S. Anterograde axonal transport of glial cell line-derived neurotrophic factor and its receptors in rat hypoglossal nerve. *Neuroscience* **97**, 575-580 (2000).

19. Thang,S.H., Kobayashi,M., & Matsuoka,I. Regulation of glial cell line-derived neurotrophic factor responsiveness in developing rat sympathetic neurons by retinoic acid and bone morphogenetic protein-2. *J. Neurosci.* **20**, 2917-2925 (2000).

20. Lee,K.F. *et al.* Targeted mutation of the gene encoding the low affinity NGF receptor p75 leads to deficits in the peripheral sensory nervous system. *Cell* **69**, 737-749 (1992).

21. Ernfors,P., Lee,K.F., Kucera,J., & Jaenisch,R. Lack of neurotrophin-3 leads to deficiencies in the peripheral nervous system and loss of limb proprioceptive afferents. *Cell* **77**, 503-512 (1994).

22. Klein,R. *et al.* Targeted disruption of the trkB neurotrophin receptor gene results in nervous system lesions and neonatal death. *Cell* **75**, 113-122 (1993).

23. Minichiello,L. *et al.* Differential effects of combined trk receptor mutations on dorsal root ganglion and inner ear sensory neurons. *Development* **121**, 4067-4075 (1995).

24. Bergmann,I. *et al.* Analysis of cutaneous sensory neurons in transgenic mice lacking the low affinity neurotrophin receptor p75. *Eur. J. Neurosci.* **9**, 18-28 (1997).

25. Arnett,M.G., Ryals,J.M., & Wright,D.E. Pro-NGF, sortilin, and p75NTR: potential mediators of injury-induced apoptosis in the mouse dorsal root ganglion. *Brain Res.* **1183**, 32-42 (2007).

26. Klein,R. *et al.* Disruption of the neurotrophin-3 receptor gene trkC eliminates la muscle afferents and results in abnormal movements. *Nature* **368**, 249-251 (1994).

27. Farinas,I., Jones,K.R., Backus,C., Wang,X.Y., & Reichardt,L.F. Severe sensory and sympathetic deficits in mice lacking neurotrophin-3. *Nature* **369**, 658-661 (1994).

28. Carroll,P., Lewin,G.R., Koltzenburg,M., Toyka,K.V., & Thoenen,H. A role for BDNF in mechanosensation. *Nat. Neurosci.* **1**, 42-46 (1998).

29. Perez-Pinera,P. *et al.* Characterization of sensory deficits in TrkB knockout mice. *Neurosci. Lett.* **433**, 43-47 (2008).

30. Chuang,H.H. *et al.* Bradykinin and nerve growth factor release the capsaicin receptor from PtdIns(4,5)P2-mediated inhibition. *Nature* **411**, 957-962 (2001).

31. Silos-Santiago,I. *et al.* Non-TrkA-expressing small DRG neurons are lost in TrkA deficient mice. *J. Neurosci.* **15**, 5929-5942 (1995).

32. Coderre,T.J., Grimes,R.W., & Melzack,R. Deafferentation and chronic pain in animals: an evaluation of evidence suggesting autotomy is related to pain. *Pain* **26**, 61-84 (1986).

33. Smeyne,R.J. *et al.* Severe sensory and sympathetic neuropathies in mice carrying a disrupted Trk/NGF receptor gene. *Nature* **368**, 246-249 (1994).

34. Jansen,P. *et al.* Roles for the pro-neurotrophin receptor sortilin in neuronal development, aging and brain injury. *Nat. Neurosci.* **10**, 1449-1457 (2007).

35. Mu,X., Silos-Santiago,I., Carroll,S.L., & Snider,W.D. Neurotrophin receptor genes are expressed in distinct patterns in developing dorsal root ganglia. *J. Neurosci.* **13**, 4029-4041 (1993).

36. Hermans-Borgmeyer,I., Hermey,G., Nykjaer,A., & Schaller,C. Expression of the 100-kDa neurotensin receptor sortilin during mouse embryonal development. *Brain Res. Mol. Brain Res.* **65**, 216-219 (1999).

37. Horton,A.C. & Ehlers,M.D. Neuronal polarity and trafficking. *Neuron* **40**, 277-295 (2003).

38. Merianda,T.T. *et al.* A functional equivalent of endoplasmic reticulum and Golgi in axons for secretion of locally synthesized proteins. *Mol. Cell Neurosci.* **40**, 128-142 (2009).

39. Kamal,A., Almenar-Queralt,A., LeBlanc,J.F., Roberts,E.A., & Goldstein,L.S. Kinesin-mediated axonal transport of a membrane compartment containing beta-secretase and presenilin-1 requires APP. *Nature* **414**, 643-648 (2001).

40. Kjolby,M. *et al.* Sort1, encoded by the cardiovascular risk locus 1p13.3, is a regulator of hepatic lipoprotein export. *Cell Metab* **12**, 213-223 (2010).

41. Jenkins,P.M., Zhang,L., Thomas,G., & Martens,J.R. PACS-1 mediates phosphorylation-dependent ciliary trafficking of the cyclic-nucleotide-gated channel in olfactory sensory neurons. *J. Neurosci.* **29**, 10541-10551 (2009).

42. Ascano,M., Richmond,A., Borden,P., & Kuruvilla,R. Axonal targeting of Trk receptors via transcytosis regulates sensitivity to neurotrophin responses. *J. Neurosci.* **29**, 11674-11685 (2009).

Figure 1

Vaegter et al. 2010
NN-A27821D

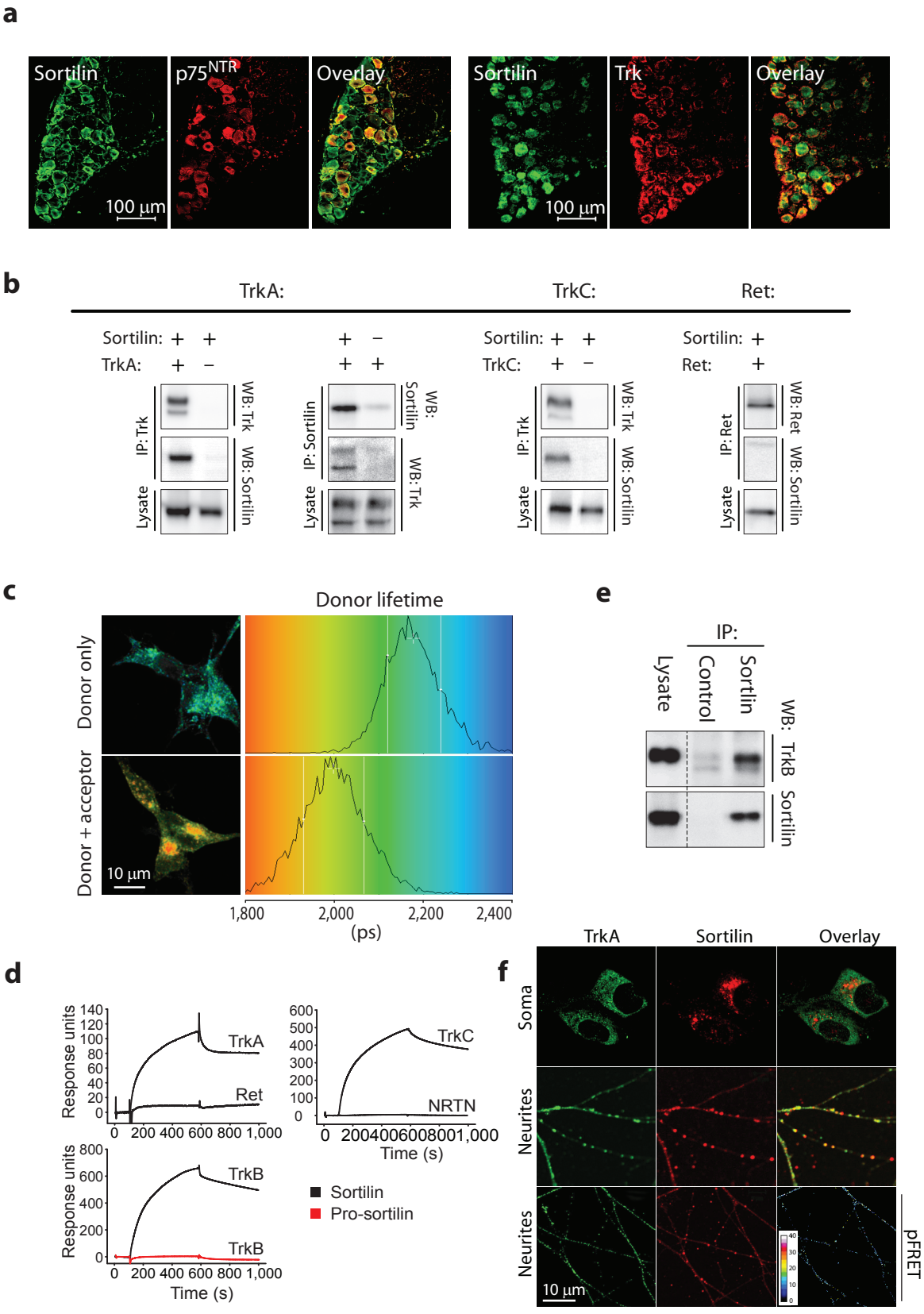

Figure 2

Vaegter et al. 2010
NN-A27821D

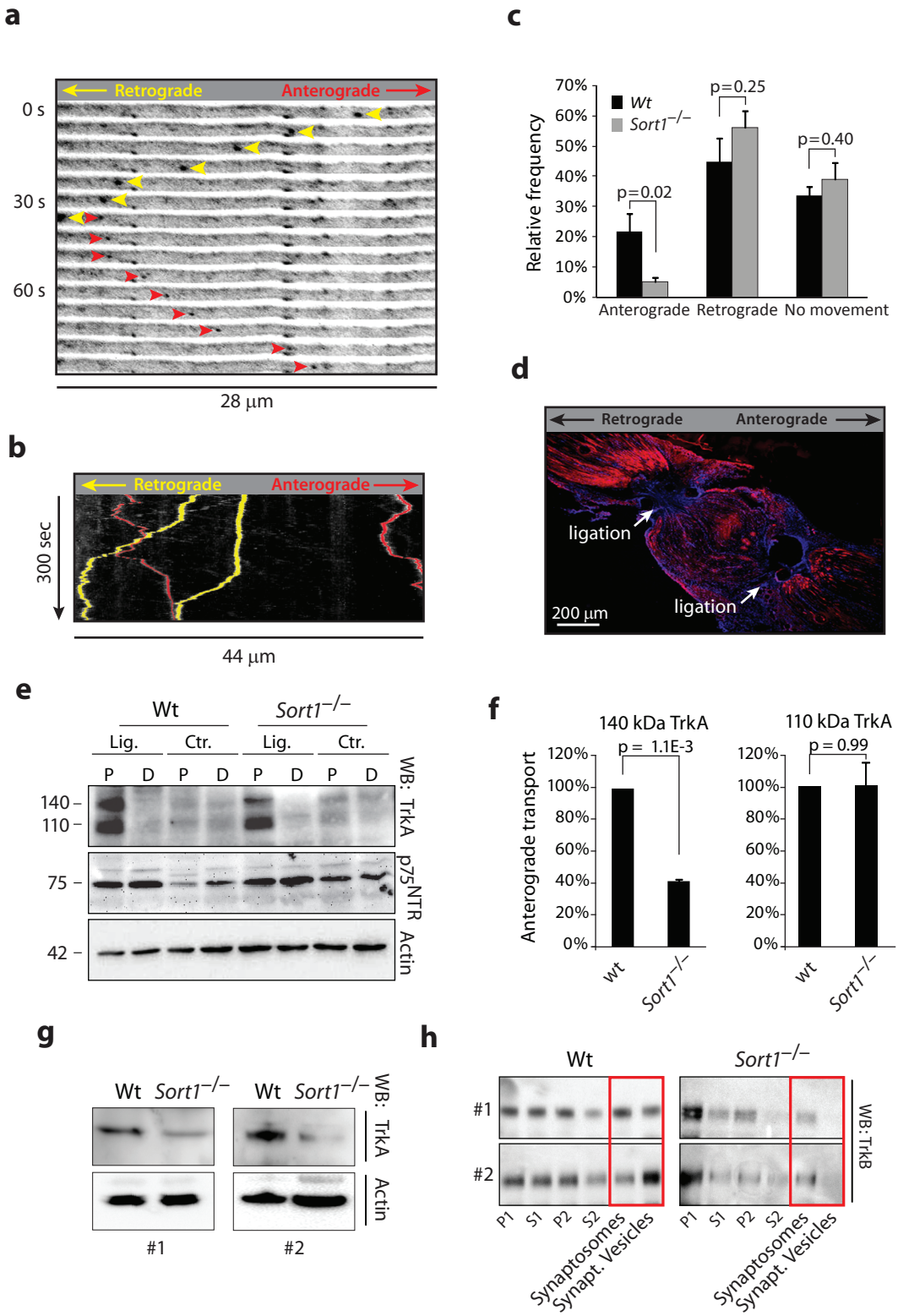

Figure 3

Vaegter et al. 2010
NN-A27821D

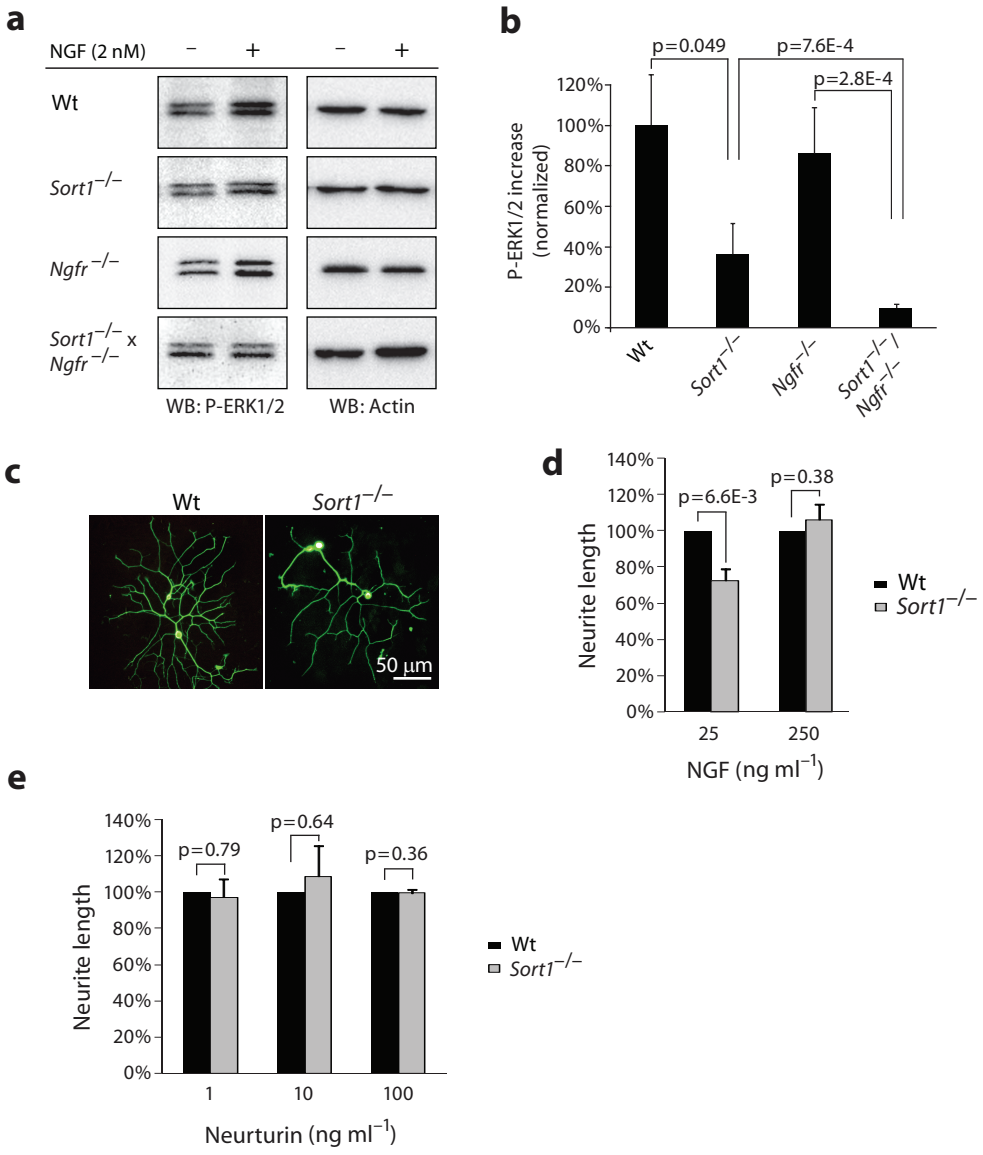

Figure 4

Vaegter et al. 2010
NN-A27821D

a

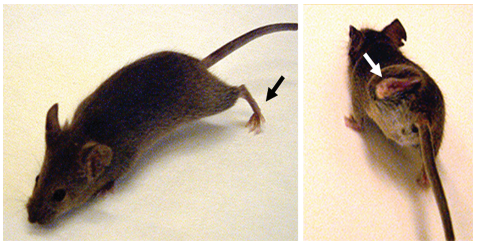

b

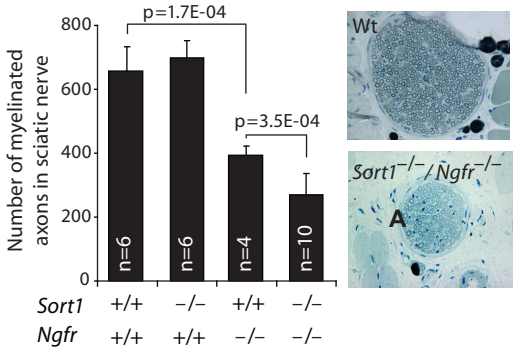

c

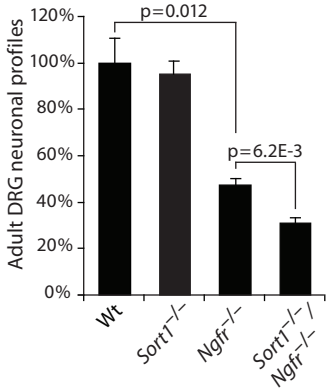

Figure 5

Vaegter et al. 2010
NN-A27821D

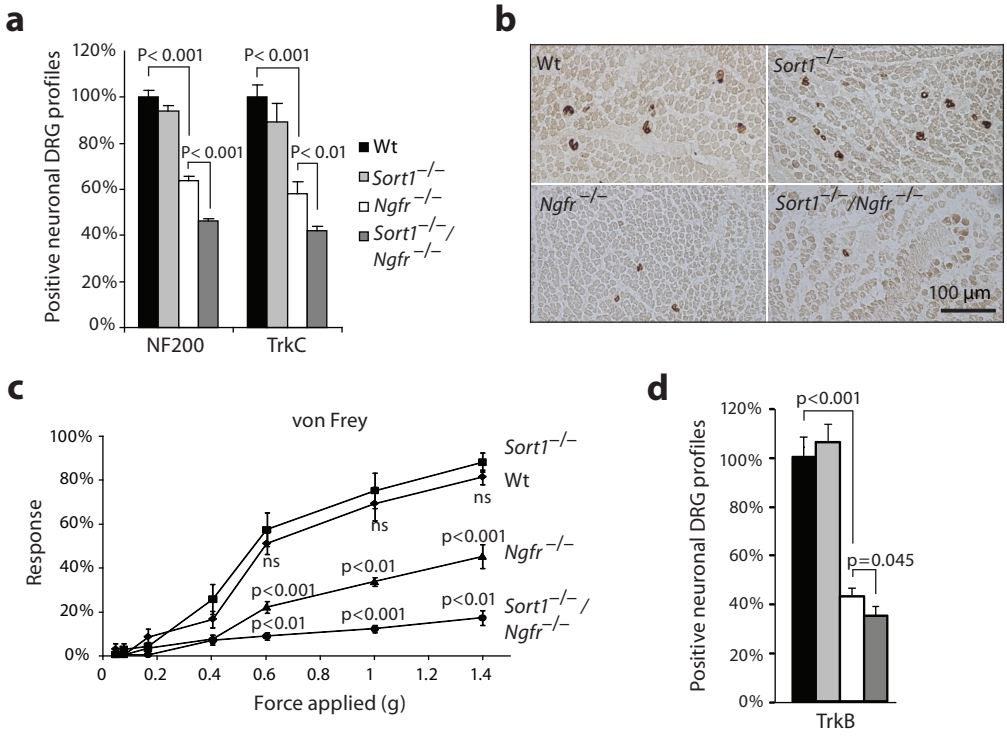

Figure 6

Vaegter et al. 2010
NN-A27821D

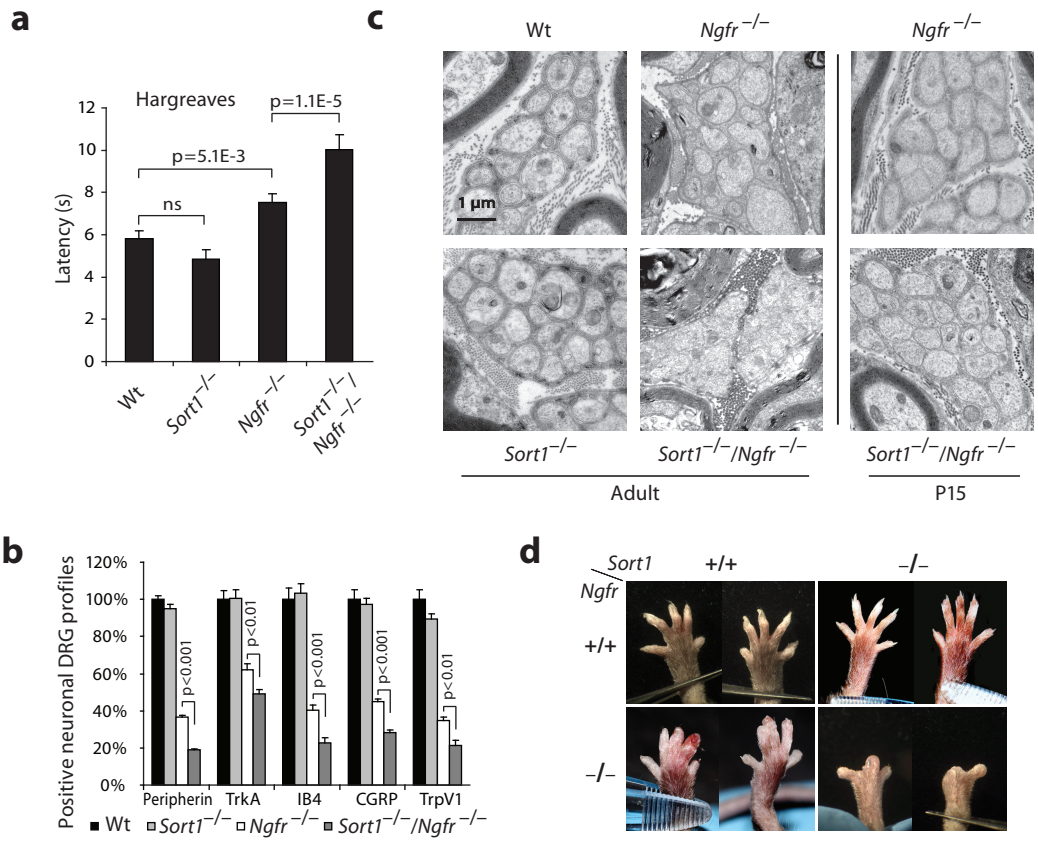

Figure 7

Vaegter et al. 2010
NN-A27821D